Korean J. Chem. Eng., 35(10), 2133-2137 (2018)
DOI: 10.1007/s11814-018-0114-9

pISSN: 0256-1115
eISSN: 1975-7220

Surface modified nanostructured-TiO_2 thin films for removal of Congo red

Alka Tiwari*, Alok Shukla*, Suk Soon Choi, and Seung-Mok Lee***,†**

*National Institute of Technology Mizoram Chaltlang, Aizawl- 706002 (Mizoram), India
**Department of Biological and Environmental Engineering, Semyung University, Jecheon 27136, Korea
***Department of Health and Environment, Catholic Kwandong University, Gangneung 25601, Korea
(*Received 2 April 2018 • accepted 26 June 2018*)

Abstract−We synthesized nanostructured TiO_2 thin films by the modified sol-gel template method using the polyethylene glycol as filler media. The TiO_2 surface modification for both the thin films, i.e., template and non-template, was done with the ascorbic acid. All the four thin film samples, S1 (TiO_2 (non-template), TiO_2 (template), S3 (S1 modified with ascorbic acid) and S4 (S2 modified with ascorbic acid), were characterized by various analytical methods. Phase evaluation was monitored by the X-Ray diffraction analysis. Moreover, the thin films particle sizes were obtained to be 22.32, 21.20, 14.52 and 16.77 nm, respectively for the samples S1, S2, S3 and S4. The changes in particle size and morphology due to the PEG and ascorbic acid were determined by scanning electron microscopy (SEM). Similarly, thermal gravimetric (TG) and differential scanning calorimetry (DSC) were performed to determine the decomposition behavior of organic compound present in the solid samples. The functional groups were determined by infrared (IR) analysis. The photocatalytic efficiency, as a reference of Congo red, was conducted using all the four samples of TiO_2 thin films. Complete photocatalytic degradation of Congo red was achieved by these samples within 130, 80, 40 and 30 mins of UV illumination.

Keywords: Nanostructured Surface Modified TiO_2, Photo Catalytic Oxidation, Congo Red

INTRODUCTION

Water pollution is the greatest threat and challenge that humanity is facing at present. A variety of human activities introduce several contaminating substances into water bodies, resulting in a deleterious effect on the quality of rivers, lakes, ground, aquifers and oceans [1-4]. A variety of water contaminants include various synthetic organic/or inorganic compounds including industrial dyes, noxious gases etc. [5-8]. The heavy metal toxic ions seemingly pose serious environmental concerns affecting significantly the water quality of water bodies [9].

Several water pollutants were found to be highly toxic and eventually showed serious health issues to living beings even at trace levels. It was demonstrated that an enhanced level of contaminated water eventually causes lesser availability of fresh water to living beings. Many developed or developing countries are facing a serious scarcity of fresh water. A rough prediction showed that by 2025, one-third of world population will live in water scarce areas [10]. Moreover, the recycled waste waters are composed of several pollutants--suspended particles, variety of bacteria/pathogens or the soluble pollutants--and were found to be difficult for efficient treatment [11].

The decontamination of polluted water is basically conducted by various treatment steps. The primary screening and removal of particulate matters is followed by the biological treatment. However, there are several contaminants which were found relatively stable that needs greater attention for its effective degradation/or elimination by using the advanced treatment process [12,13]. Chlorination is widely used for disinfection of contaminated water; however, the by-products formed, hypohalous compounds, are found to be mutagenic and carcinogenic [14-16]. On the other hand, the advanced oxidation processes (AOPs) using the suitable photocatalyst for degradation of stable organic compounds present in wastewater are well accepted processes, and several studies have demonstrated how to utilize effectively the AOP process to meet the stringent regulatory guidelines of safe water [17,18]. The AOPs treatments are performed with *in situ* production of radicals, H_2O_2, ·OH, O_2, O_3, which readily mineralizes the stable organic contaminants [19,20]. The role of hydroxyl radical was, although, found less selective for water contaminants. The radical readily degrades many stable contaminants that are dissolved in water [21,23].

Therefore, the process of AOPs contained with heterogeneous photo-catalysts including titanium dioxide has shown fairly good efficacy in removing a variety of stable pollutants to its possible biodegradable products. In a word, TiO_2 shows efficient photo-catalytic performance operated with radiation energy wavelength 300-390 nm. Moreover, photo-catalysis is not only employed in water treatment; however, the process is increasingly employed in air purification, self-cleaning solid surfaces etc. [24]. The fundamentals of photo-physics and photo-chemistry using the semiconductor TiO_2 catalyst was utilized extensively [25,26]. The semiconductor TiO_2 photo-catalyst induces a series of redox processes on its solid surfaces [27].

However, the presence of dissolved oxygen (DO) in water bodies plays an important role in the degradation of water contaminants. Devoid of DO and water molecules restricted greatly the

†To whom correspondence should be addressed.
E-mail: leesm@cku.ac.kr

generation of hydroxyl radicals (·OH) [28].

Titanium dioxide mainly exists in the crystalline phases: rutile, anatase and brookite. Further, rutile and anatase have shown potential application in photocatalytic implications. Overall, the photocatalytic property of TiO_2 was demonstrated based on the crystallinity of solid, specific surface area of catalyst, number of surface hydroxyl groups, point of zero charge of catalyst, defects in crystal etc. [29]. The anatase phase of TiO_2 eventually showed an enhanced efficiency in photocatalytic operations; however, the rutile phase was found to be effective in various redox processes [30].

TiO_2 is widely employed either as dispersed fine particles in polluted aqueous medium [31] or as impregnated on suitable solid substrate [32,33]. Recently, a report showed that TiO_2 nanoparticles possessed potential photo-toxicity towards the *Oryzias latipes* embryos and sac-fry exposed to different irradiation conditions [34]. However, this problem was overcome by employing the impregnated TiO_2 on different substrates. The impregnation of TiO_2 was obtained by chemical vapor deposition [35], chemical spray pyrolysis [36], electrodeposition [37] and sol-gel dip coating methods [32]. This method is carried out preferably by hydrolysis and polycondensation of titanium alkoxide, which results in gel formation. Further annealing of sol gives an ordered crystalline network of TiO_2 [38, 39]. Catalytic performance is improved significantly by using porous solid materials. The mesoporous TiO_2 thin film was synthesized by template synthesis using polyethylene glycol as filler media [40]. The surface modification of TiO_2 could further enhance its suitability in photocatalytic operations [41]. In principle, surface modifiers play an important role in catalyst performance by reducing significantly the electron hole pair recombination, enhancing the wavelength responses or even the selectivity of catalyst.

Therefore, the aim of the present study was to synthesize the porous TiO_2 film, using the polyethylene glycol (a template), on solid substrate (borosilicate glass) by adopting sol-gel dip impregnation method and surface modification of TiO_2 thin films with L(+)-ascorbic acid (AA). The photocatalytic efficiency of these thin films was investigated using a reference water contaminant, Congo red.

EXPERIMENTAL

1. Preparation of TiO_2 Precursor Sol

Two different TiO_2 precursor sols were prepared: Sol 1 and Sol 2. Sol 1 was prepared by dissolving 11.10 g of titaniumisopropoxide (TTIP) in 100 ml of absolute ethyl alcohol under continuous stirring. A drop of acetic acid (3 M) was added to the precursor titanium isopropoxide solution and it was ultra-sonicated for 12 mins and the solution was aged for 12 hrs. Sol 2 was prepared using the same procedure as the one described for Sol 1 except that 2 g of polyethylene glycol (PEG) was added simultaneously with titanium precursor solution.

2. Preparation of Thin Film

The clean and dried borosilicate glass plates were immersed in to the Sol 1 and Sol 2 solution at a control speed and remained dipped for 1 hr. It was removed carefully and placed in air at room temperature for 12 hrs. TiO_2 was aggregated on to the substrate and formed a thin film on it. The solvent was evaporated at 100 °C for 1 hr and then fired at 500±1 °C for 3 hrs in an electric furnace. The immersing of glass plate was repeated for another three times for both sol solutions separately in order to obtain the desired thin uniform film onto the borosilicate glass.

The remaining amount of solutions (Sol 1 and Sol 2 named as S1 and S2) was centrifuged for 20 mins. At 8,000 rpm to remove water and ethyl alcohol and were dried at 100 °C for 48 hrs in order to obtain dried gel powders.

3. Surface Modification

The TiO_2 thin films were prepared by using the Sol 1 (S1) and Sol 2 (S2). The disks were dipped into the aqueous solutions of ascorbic acid (AA) for 10 mins, resulting in a deep orange color of the surface. These films were heat-treated for 30 mins at 120 °C to eliminate physisorbed water and the obtained samples were named as S3 and S4, respectively. The color developed implies that a chemical bond was formed between the ascorbic acid and TiO_2 (chemisorption) [41]. The films were then removed, thoroughly rinsed in a dilute acidic aqueous solution and washed repeatedly with distilled water. They were then stored in an argon atmosphere until employed for catalytic activity.

4. Characterization

The crystallinity of the TiO_2 films was obtained by X-ray diffraction (XRD) using Philips powder diffractometer with Cu-K_α radiations. The surface morphology of TiO_2 films was observed using scanning electron microscopy (SEM, Philips XL-20) with an accelerating voltage of 20 kV. The thermal properties of the TiO_2 samples were carried out by means of thermo gravimetric/differential scanning calorimetry TG/DSC.

5. Photocatalytic Degradation Experiments

The photocatalytic degradation was carried out in the batch reactor experimentation. A black box was arranged and inside the LED based sensor was used to detect the degradation of Congo red (Congo red, which is water soluble yielding a red colloidal solution). 40.0 mg/L of commercial Congo red was dissolved in distilled water and used for its photocatalytic degradation. The increase in concentration of Congo red caused for decrease in potential.

RESULTS AND DISCUSSION

1. Characterization of Solid Samples

The SEM images are presented in Fig. 1. Fig. 1 clearly shows that the thin film surface obtained by S1 and S2 samples appears as a plain and smooth uniform surface. However, it is clear that the wide pore size distribution was appreciably more pronounced in S3 and S4 than S1 and S2 samples. This indicates that that the S3 and S4 samples possessed an enhanced surface roughness and heterogeneity. Rough and more porous surface plays a useful role in the photocatalytic activity since the photocatalytic reaction occurs at the surface and a larger surface area is expected to provide more photocatalytic reactions to take place. In comparison, the S4 sample could be accountable to provide larger surface area for more photocatalytic reactions, and a slightly higher photocatalytic activity than S3 sample.

The crystallinity of the photocatalysts was analyzed by the X-ray diffractometer obtained by X-ray diffraction (XRD) data. The analysis was carried out using Cu-K_α radiations operated at 40 kV and 250 mA at scanning angle (2θ) ranging from 5° to 80° at a scanning

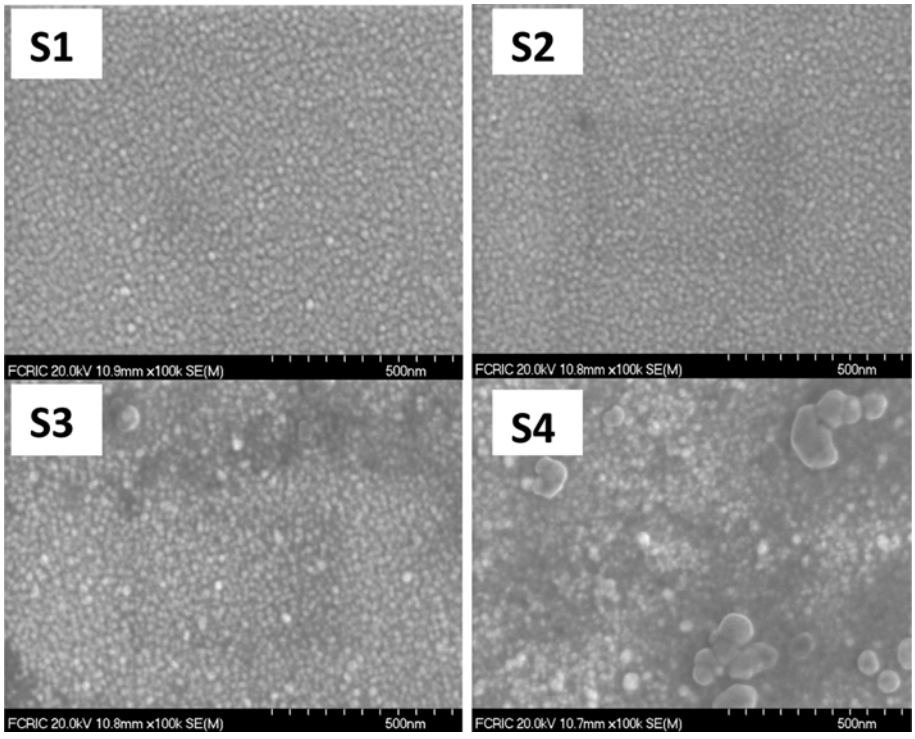

Fig. 1. SEM images of TiO_2 thin films S1, S2, S3 and S4 obtained on borosilicate glass substrates.

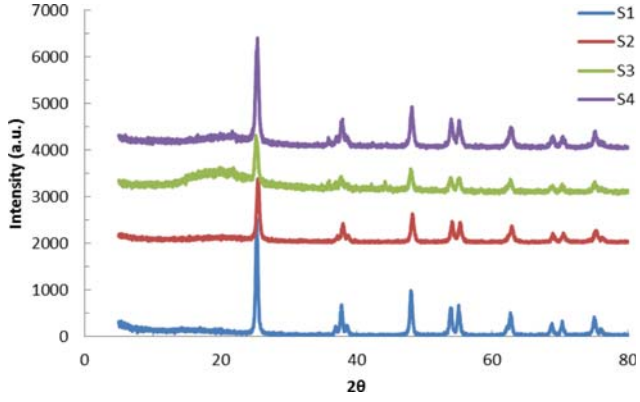

Fig. 2. X-ray diffraction pattern of TiO_2 thin films S1, S2, S3 and S4.

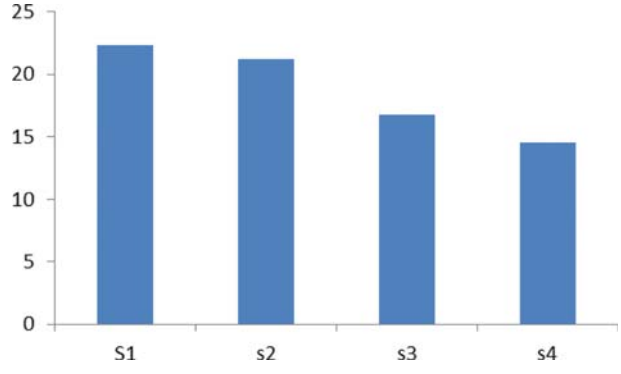

Fig. 3. Particle size distribution of various TiO_2 thin film samples.

rate of 4° min^{-1}. Fig. 2 shows the XRD patterns of the calcined TiO_2 thin films: S1, S2, S3 and S4. The anatase phase was the predominant structure of these thin films. This indicates that all TiO_2 thin films are composed with a single crystalline anatase phase since the characteristic peaks occurred at the 2θ values of 25.4, 38, 48, 54, 55, and 63. Rutile and brookite phases were apparently absent in these thin films.

The particle diameter of titanium dioxide was calculated by the Debye-Scherrer Eq. (1):

$$D = \frac{8.9x\lambda}{B\cos\theta} \quad (1)$$

where λ is the incident X-rays wavelength, B and θ are the full width at half maxima (FWHM) and semi-angle of diffraction corresponding to the most intensive diffraction peak, respectively. [42].

Fig. 3 shows that the particle sizes of the four different TiO_2 thin film samples were 22.32, 21.20, 16.77 and 14.53 nm, respectively, for the S1, S2, S3 and S4 samples. The thin film obtained by the template PEG had relatively lower particle sizes, whereas the surface modified samples, S3 and S4, further showed lower particle size distribution compared to the unmodified S1 or S2 thin films. Small particle size of thin films perhaps possesses enhanced specific surface area and shows efficient photocatalytic activity.

Fig. 4 shows the TG curves of the synthesized TiO_2 samples. The weight loss of all samples occurred in two stages. First weight loss peak was observed between 139 °C to 150 °C, and second peak was between 238 °C to 246 °C. These two peaks of weight loss appeared due to the evaporation of absorbed water and ethanol in the titania gels and the combustion of unhydrolyzed isopropoxide ligands or the evaporation of other organic substances bonded to nanotitania particles. This further conformed to the exothermic processes by

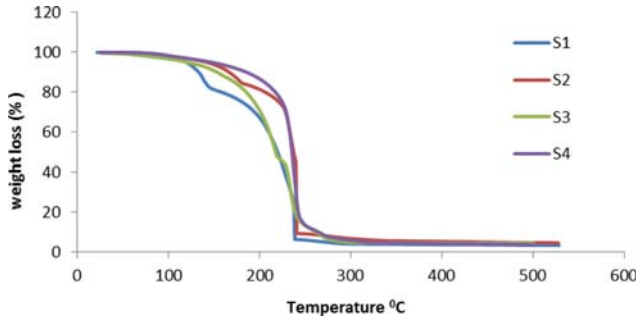

Fig. 4. TG curves of various TiO_2 samples.

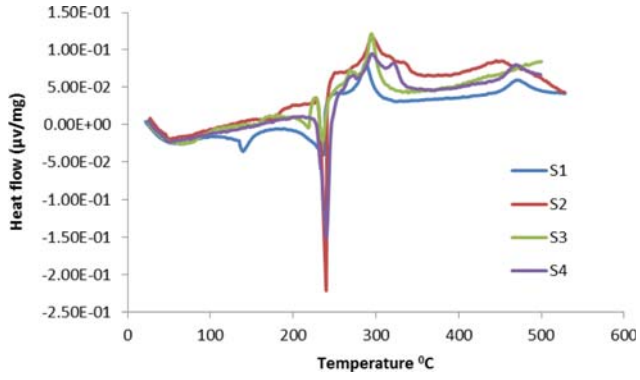

Fig. 5. DSC curves of various TiO_2 samples.

the DSC curves also.

Similarly, Fig. 5 shows the DSC curves of all these TiO_2 samples. The figure clearly evidences two main exothermic processes, which is almost identical for all the samples, i.e., S1, S2, S3 and S4. The viewed difference is only the peak size. It further demonstrates that the exothermic process is completed for all samples around 500 °C. The first exothermic peak is due to the evaporation of absorbed water and ethanol and release of organic substances. The transformation of the amorphous phase to the anatase phase showed the second exothermic peak.

Fourier transform-infra red (FT-IR) results were obtained for the TiO_2 solids S1, S2, S3 and S4 and illustrated in Fig. 6. Note that the IR results are almost similar for these solids. A sharp vibrational band occurred around the wave number 3,436 cm^{-1} due to

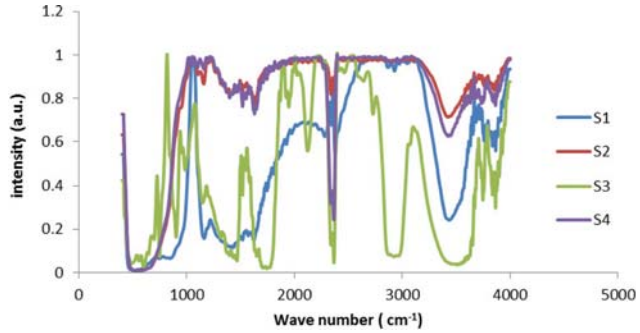

Fig. 6. FT-IR spectra of various TiO_2 samples.

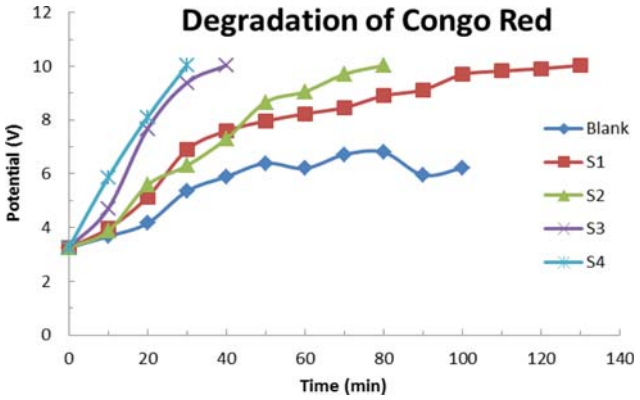

Fig. 7. Photocatalytic degradation of Congo red using different synthesized TiO_2 thin film samples.

the stretching vibrations of O-H present with Ti-OH [43]. Similarly, the bending vibration of O-H appeared around 1,637 cm^{-1}. On the other hand, IR absorption bands occurring around 471 and 421 cm^{-1} were clearly due to the bending vibrations of Ti-O and Ti-O-Ti [44] or possibly due to stretching vibrations of Ti-O [45]. Additionally, vibrational peaks around 2,920 and 2,861 cm^{-1} occurred because of the presence of ascorbic acids present with the TiO_2 matrix [46]. This eventually confirms the presence of ascorbic acid on the surface.

2. Photocatalytic Performance of TiO_2 Thin Films

The photocatalytic behavior of these TiO_2 thin films, S1, S2, S3 and S4, was assessed using the UV-illumination in the possible removal of Congo red. The Congo red solution (40.0 mg/L) was intended to degrade using these thin film samples photocatalysts. A blank was also carried out using the Congo red (40.0 mg/L) and with bare borosilicate glass and illuminated with UV light. Results were recorded as a function of time and returned in Fig. 7. It is clearly observed that very slow and incomplete degradation occurred with bare silica glass (blank). However, a complete degradation occurred with the S1, S2, S3 and S4 with the time taken, respectively, 130, 80, 40 and 30 mins. The results clearly indicate that the catalytic performance of these thin films was in the order of S4>S3>S2>S1. The surface-modified thin film shows remarkably high degradation efficiency, and just within 20 mins of contact a complete removal of Congo red was obtained. The thin films samples can further be employed for their wider implications in the treatment of wastewaters contaminated with a variety of pollutants, including the emerging water contaminants. Previously, it was reported that the CuO nanoparticles synthesized using a silk fibroin template followed the pseudo-first order rate equation in the photocatalytic degradation of Congo red [47].

CONCLUSION

Nanostructured TiO_2 thin films samples were synthesized using the filler media as polyethylene glycol (PEG). The thin film TiO_2 samples S1 (without template) and S2 (with template) were surface modified with ascorbic acid to obtain the thin film TiO_2 samples S3 and S4, respectively. It was observed that these thin film TiO_2 samples i.e., S1, S2, S3 and S4, all had distinct anatase phase.

The SEM images of the samples showed that S1 and S2 samples were having very ordered nanosized particles, whereas samples S3 and S4 were very disordered and had micro to meso-pores on its surfaces. The particle sizes of the four different TiO_2 thin film samples were found to be 22.32, 21.20, 16.77 and 14.53 nm, respectively, for the S1, S2, S3 and S4 samples. Further, the photo-catalytic behavior of these samples showed that the degradation efficacy followed the order S4>S3>S2>S1. The TG data indicated these materials possessed two distinct peaks at the temperature range 139 °C to 150 °C and 238 °C to 246 °C, referring to the evaporation of absorbed water and ethanol molecules with the titania and the combustion of unhydrolyzed isopropoxide ligands or the evaporation of other organic substances bonded to the nanotitania particles, respectively. The photocatalytic efficiency of these TiO_2 thin films showed the order S4>S3>S2>S1 in the degradation of Congo red from aqueous solutions. A complete degradation of Cong red was achieved just within 20 mins of contact using the S4 thin film samples. These preliminary experiments further pave the way to utilizing the thin film samples in the large-scale treatment of wastewater even contaminated with emerging water pollutants.

ACKNOWLEDGEMENT

This research was supported by Basic Science Research Program through the National Research Foundation of Korea (NRF) funded by the Ministry of Education, Science and Technology (NRF-2017R1D1A3B03027955).

REFERENCES

1. T. Wintgens, F. Salehi, R. Hochstrat and T. Melin, *Water Sci. Technol.*, **57**, 99 (2008).
2. S. Suarez, M. Carballa, F. Omil and J. M. Lema, *Rev. Environ. Sci. Bio-Technol.*, **7**, 125 (2008).
3. A. A. Babaei, B. Kakavandi, M. Rafieed, F. Kalantarhormizi, I. Purkaram, E. Ahmadi and S. Esmaeili, *J. Ind. Eng. Chem.*, **56**, 163 (2017).
4. A. Khan, S. M. Prabhu, J. Park, W. Lee, C.-M. Chon, J. S. Ahn and G. Lee, *J. Ind. Eng. Chem.*, **47**, 86 (2017).
5. D. Bahnemann, *Solar Energy*, **77**, 445 (2004).
6. A. Vidal, *Chemosphere*, **36**, 2593 (1998).
7. M. K. Kim and K. D. Zoh, *Environ. Eng. Res.*, **21**, 319 (2016).
8. J. Singh, Y. Y. Chang, J. R. Koduru, J. K. Yang and D. P. Singh, *Environ. Eng. Res.*, **22**, 245 (2017).
9. R. Vinu and G. Madras, *J. Ind. Insti. Sci.*, **90**, 189 (2010).
10. J. Ganoulis, Risk Analysis of Water Pollution, 2nd Ed. *WILEY-VCH*, **Chapt. 1**, 1 (2009).
11. J. W. Viessman and M. J. Hammer, Water Supply and Pollution Control, sixth Ed. Addison Wesley Longman Inc., California U.S.A. (1998).
12. A. Garcia, A. M. Amat, A. Arques, R. Sanchis, W. Gernja and M. I. Maldonado, *Environ. Chem. Lett.*, **3**, 169 (2006).
13. P. V. A Padmanabhan, K. P. Sreekumar, T. K. Thiyagarajan, R. U. Satpute, K. Bhanumurthy, P. Sengupta, G. K. Dey and K. G. K. Warrier, *Vacuum*, **80**, 11 (2006).
14. H. Yang and H. Cheng, *Sep. Purif. Technol.*, **56**, 392 (2007).
15. J. Lu, T. Zhang, J. Ma and Z. Chen, *J. Hazard. Mater.*, **162**, 140 (2009).
16. H. M. Coleman, C. P. Marquis, J. A. Scott, S. S. Chin and R. Amal, *Chem. Eng. J.*, **113**, 55 (2005).
17. S. M. Rodriguez, J. B. Galvez and C. A. E. Gasca, *Solar Energy*, **77**, 443 (2004).
18. M. Franch, J. A. Ayllón and X. Domènech, *Appl. Catal., B: Environ.*, **50**, 89 (2004).
19. S. Esplugas, J. Gimenez, S. Conteras, E. Pascual and M. Rodrıguez, *Water Res.*, **36**, 1034 (2002).
20. R. Ahmad, R. S. Singh and B. Pal, *J. Ind. Eng. Chem.*, **37**, 288 (2016).
21. Y. Jiang, F. Li, Y. Liu, Y. Hong, P. Liu and L. Ni, *J. Ind. Eng. Chem.*, **41**, 130 (2016).
22. M. Pera-Titus, V. Garcia-Molina, M. A. Banos, J. Gimenez and S. Esplugas, *Appl. Catal., B: Environ.*, **47**, 219 (2004).
23. R. Andreozzi, V. Caprio, A. Insola and R. Marotta, *Catal. Today*, **53**, 51 (1999).
24. J. M. Herrmann, *Catal. Today*, **53**, 115 (1999).
25. U. I. Gaya and A. H. Abdullah, *J. Photochem. Photobiol. C: Photochem. Rev.*, **9**, 1 (2008).
26. A. Fujishima, T. N. Rao and D. A. Tryk, *J. Photochem. Photobiol. C: Photochem.*, **1**, 1 (2000).
27. S. Sorcar, A. Razzaq, H. Tian, C. A. Grimes and S.-I. In, *J. Ind. Eng. Chem.*, **46**, 203 (2017).
28. J. A. Byrne and B. R. Eggins, *J. Electroanal. Chem.*, **457**, 61 (1998).
29. N. Serpone, *J. Photochem. Photobiol. A*, **104**, 1 (1997).
30. N. Park, J. Van de Lagemaat and A. J. Frank, *J. Phys. Chem. B*, **104**, 8989 (2000).
31. A. Yasumori, K. Yamazaki, S. Shibata and M. Yamane, *J. Ceram. Soc. Jpn.*, **102**, 702 (1994).
32. R. S. Sonawane, S. G. Hedge and M. K. Dongare, *Mater. Chem. Phys.*, **77**, 744 (2002).
33. S. H. Nam, Y. J. Shin and Y. J. An, *Environ. Eng. Res.*, **22**, 426 (2017).
34. J. A. Mendoza, D. H. Lee and J. H. Kang, *Environ. Eng. Res.*, **21**, 291 (2016).
35. P. G. Karlsson, J. H. Richter, M. P. Andersson, M. K. J. Johansson, J. Blomquist, P. Uvdal and A. Sandell, *Surf. Sci.*, **605**, 1147 (2001).
36. A. Lopez, D. Acosta, A. Martínez and J. Santiago, *Powder Technol.*, **202**, 111 (2010).
37. Y. Ishikawa and Y. Matsumoto, *Electrochim. Acta*, **46**, 2819 (2001).
38. M. Keshmiri, M. Mohseni and T. Troczynski, *Appl. Catal., B: Environ.*, **53**, 209 (2004).
39. Y. Chen, E. Stathatos and D. D. Dionysiou, *J. Photochem. Photobiol. A: Chem.*, **203**, 192 (2009).
40. N. Arconada, A. Durán, S. Suárez, R. Portela, J. M. Coronado, B. Sánchez and Y. Castro, *Appl. Catal., B: Environ.*, **86**, 1 (2009).
41. A. P. Xagas, M. C. Bernard, A. Hugot-Le Goff, N. Spyrellis, Z. Loizos and P. Falaras, *J. Photochem. Photobiol. A: Chem.*, **132**, 115 (2000).
42. L. Lopez, W. A. Daoud and D. Dutta, *Surf. Coatings Technol.*, **205**, 251 (2010).
43. S. Rahim, M. S. Ghamsari and S. Radiman, *Scientia Iranica F*, **19**, 948 (2012).
44. J. Maira, J. M. Coronado, V. Augugliaro, K. L. Yeung, J. C. Conesa and J. Soria, *J. Catal.*, **202**, 413 (2001).
45. L. G. Devi and K. M. Reddy, *Appl. Surf. Sci.*, **257**, 6821 (2011).
46. S. Sugapriya, R. Sriram and S. Lakshmi, *Optik*, **124**, 4971 (2013).
47. J. W. Kim, C. S. Ki, I. C. Um and Y. H. Park, *J. Ind. Eng. Chem.*, **56**, 335 (2017).